



11th conference of the International Sports Engineering Association, ISEA 2016

Explicit finite element methods for equestrian applications

Karin Brolin*, Jacob Wass

Department of Applied Mechanics, Centre for Sports and Technology, Chalmers University of Technology, 412 96 Göteborg, Sweden

Abstract

A virtual human body model (HBM), developed for vehicle crash simulations, was used to conduct a pilot study of dangerous accidents that occur in equestrian sports. It was performed to illustrate the potential that the explicit finite element (FE) HBMs have to improve rider safety and to assess the protective capacity of the safety vest. Four different questions were addressed:

1. When a rider is trampled by a horse, how does the risk of injury vary with chest impact location?
2. Does a safety-vest provide protection if the rider is kicked by a horse and does the protection vary with the violence of the hoof impact?
3. Can a safety-vest provide any benefit when the rider is hit by the horse after a rotational fall?
4. How does the risk for thoracic injuries vary when the rider falls off the back of a horse at different angles?

The HBM was the Total Human Model for Safety AM50 version 3.0 (Toyota Motor Corporation, Japan), improved for thorax injury predictability in a previous automotive project. The FE code was LS-DYNA (Livermore Software Technology Corporation, USA). Models of a generic safety vest, a horse impactor and a hoof were developed as part of this project. The risk of thorax injury was evaluated with stresses and strains measured for each rib, and the chest deformation criteria D_{max} and D_{cTHOR} .

The following results were obtained for each question:

1. The risk of injury was higher for hoof impacts close to the sternum compared to more lateral locations that had up to 25% less risk. Hence, this knowledge could be used to optimize novel safety-vest designs with HBM simulations.
2. Yes, the safety-vest provided protection against horse kicks, and it varied with the violence of the kick. Therefore, if the range of impact energy that occurs in real-world accidents is known, HBM simulations can be used to optimize the vest material properties.
3. No, the safety-vest did not provide any benefit when the horse lands on top of the rider. This conclusion suggests that safety measures should focus on preventing this type of accident, rather than designing personal protection for the rider.
4. When the rider falls with the head first, the number of predicted rib fractures increases compared to flat falls. However, the model predicts rib fractures for all of the falls simulated from a height of 1.5 meters for a rider without a safety vest.

To conclude, FE HBMs have the potential to improve equestrian safety and further studies on equestrian safety-vests designs are warranted.

© 2016 The Authors. Published by Elsevier Ltd. This is an open access article under the CC BY-NC-ND license (<http://creativecommons.org/licenses/by-nc-nd/4.0/>).

Peer-review under responsibility of the organizing committee of ISEA 2016

Keywords: Equestrian; Safety; Rib fractures; Finite element; Chest;

1. Introduction

Equestrian sports are popular and have a high incidence of injuries and fatalities compared to other sports. A recent review of the literature states that the most leading cause for rider injuries were fall accidents, followed by horse kicks or being stepped on by the horse [1]. In equestrian trauma, the most frequently injured body areas are reported to be the head, extremities and chest [1-3], their order of appearance changes depending on the study design. A US study [3] found that the injury patterns varied with age, where the most frequent injury for children (below 18 years of age) were upper extremity fractures, for younger adults (19 – 49 years of age) were concussion, and for older adults (above 50 years of age) were rib fractures. Wearing a riding helmet has been shown to be beneficial to reduce the head injury severity [3]. However, to the best knowledge of the authors, there is no study on

* Corresponding author. Tel.: +46-31-7721509. E-mail address: karin.brolin@chalmers.se

the protective capacity of the safety-vests for riding that shows a safety benefit. There are many different safety-vest designs on the market and they are very likely to have a significant difference in safety benefit. Hence, there is a need to assess the protective capacity of safety-vests for riding.

Safety interventions can be assessed with real-world data (epidemiological studies). The major drawback is that the products must have been on the market some time before they show up in accident statistics. Ideally, the safety should be assessed before the products are launched on the market, to avoid preventable injuries due to faulty or less-efficient safety devices. In automotive safety, accident statistics are complemented with physical and virtual crash testing. Safety interventions and principles are evaluated with human substitutes, such as crash test dummies. Nowadays, most product development is done virtually and safety is assessed with virtual crash testing using explicit finite element (FE) simulations. Therefore, there have been many international research efforts to create biofidelic human body models (HBMs) that are validated to predict injury due to impact loading. These models are promising to study other impact scenarios, such as equestrian accidents.

This pilot study aims to assess the potential that FE HBMs have to improve rider safety with respect to thoracic injuries and to evaluate the protective capacity of a safety vest. Four different questions were chosen based on the relevance to rider safety:

1. When a rider is trampled by a horse, does the risk of injury vary with chest impact location?
2. Does a safety-vest provide protection if the rider is kicked by a horse and does the protection vary with the violence of the hoof impact?
3. Can a safety-vest provide any benefit when the horse lands on top of the rider after a fall?
4. How does the risk for thoracic injuries vary when the rider falls off the back of a horse at different angles?

2. Method

All simulations were performed with the FE solver LS-DYNA (LSTC Inc., Livermore, CA, USA), surface processing was done with CATIA version 5 (3DS Dassault Systèmes, Paris, France), meshing with Hypermesh (Altair Engineering, Troy, MI, USA), and post-processing with LS-PREPOST (LSTC Inc., Livermore, CA, USA) and MATLAB (The Mathworks Inc., Natick, MA, USA). The HBM used was the Total Human Model for Safety AM50 version 3.0 (Toyota Motor Corporation, Japan), subsequently improved and validated for thoracic response [4], hereafter called THUMS.

The risk for thorax injury was evaluated with previously developed risk curves for an older population [5-6] focusing on abbreviated injury scale (AIS) 2+ injuries, i.e. two or more rib fractures. Four different criteria were used; the shear stress (τ) and maximum principal strain (ϵ_1) in the rib cortical bone, the maximum chest deflection (Dmax) [7] and differential deflection criterion (DcTHOR) [8]. Dmax measures the maximum relative chest deflection at five points on the ribcage, where 100% means that the chest was completely compressed at some point and 0% means no compression. DcTHOR measures the maximum deformation between the same points as Dmax, but with emphasis on asymmetric deformation by adding terms measuring differences in deflection between the left and right side of the ribcage. The nodes used for the displacement measures were mid sternum (#89213524), upper left (#89200050), lower left (#89206698), upper right (#89220050), lower right (#89226698) and ninth thoracic vertebra (#8913156), according to [5].

2.1. Created models

The horse hoof was modelled as an oval shaped rigid shell plate (135 x 140 mm). A mass of 125 kg was added to the hoof, which represents a fourth of the mass of a 500 kg horse.

A simplified model of a safety-vest (Fig. 1), typical of those worn by horse riders [9], was created with a foam core (thickness 20 mm) of solid hexahedral elements. It was covered by an inner and an outer surface nylon fabric (thickness 0.5 mm) of shell elements, with nodes merged to the foam core. The inner nylon fabric was meshed based on the THUMS external torso geometry to provide a perfect fit. Two layers of solid elements were offset from the inner surface to mesh the foam core. The outer nylon fabric was created on the outer faces of the foam core elements. The nylon fabric was modelled as a linear elastic material and the foam core was modelled as a low-density foam (Fig. 2). Material data are listed in Table 1, and were taken from online sources [10, 11]. A sliding contact was defined between THUMS' chest and the vest.

Table 1. Material properties for the simplified safety-vest model.

Material	LS-DYNA material model [1]	Density [kg/mm ³]	Young's modulus [GPa]	Poisson's ratio	Stress-strain relationship	Ref.
Foam core	MAT_057	2.40e-7	-	-	Linear	[10]
Nylon fabric	MAT_001	1.00e-6	2.00	0.32	Fig. 2	[11]



Fig. 1. Simplified model of a safety-vest for horse riders.

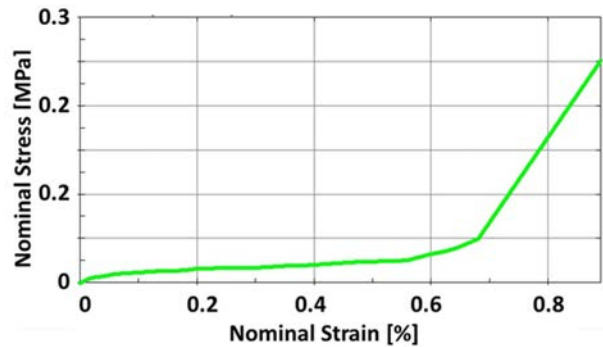


Fig. 2. Nominal stress versus strain function in the foam core material model.

The geometry for a simplified model of a horse body was created by generating the outer shape of a horse as seen from the side with splines and sweeping an oval section along the profile. The model was meshed with tetrahedron elements and given viscoelastic material properties (LS-DYNA material model MAT_006) with parameters equal to the THUMS' bulk flesh material. The density was set to $1.00e-6 \text{ kg/mm}^3$ to give a total horse mass of 500 kg.

2.2. Simulations

To predict the human chest response to horse trample at different chest impact locations, THUMS was placed above a rigid plane representing the ground (Fig. 3a). A contact was defined between the ground and THUMS' back and gravity was applied. The legs were not included in the simulation because they were considered to have little or no influence on the results of interest. The hoof model was given an initial velocity of 1 m/s directed towards the chest. Six simulations were run with different chest impact locations (Fig. 3b-c). Two locations were on the sternum: location 3 was between the second costal notches and location 6 between the fourth costal notches. Four more locations were added by applying rotations around the spine (Fig. 3b-c).

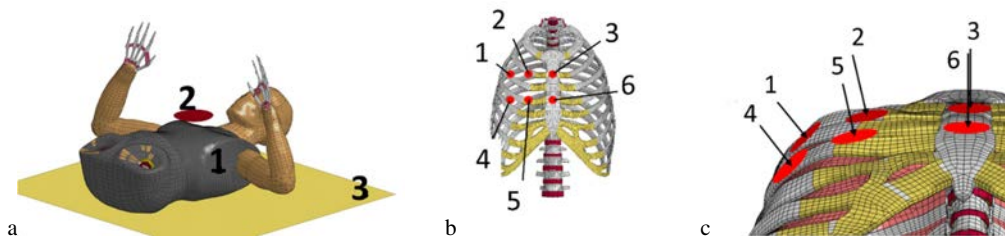


Fig. 3. (a) THUMS (1) setup to simulation a trample by a horse hoof (2) and placed with its back in contact with a rigid wall representing the ground (3), lower extremities were excluded; (b) THUMS ribcage with hoof impact locations 1-6 marked with red dots; (c) Impact angles illustrated with arrows for each location in an inferior view of the rib cage.

To simulate the chest response of riders subjected to horse kicks of different degrees of violence, THUMS, with and without the safety-vest model, was positioned vertically without back support. Gravity was not included as there was no ground contact. The hoof model was directed towards chest location 6 (Fig. 3b-c). The momentum of the hoof was varied such that the mass was constant at 125 kg and the velocity changed from 0.6 m/s up to 4.0 m/s. This range of velocities gave an investigated momentum range from 75 - 500 Ns, in steps of 25 Ns, resulting in 18 simulations.

Two simulations were performed to predict the chest response when a horse lands on top of the rider after a so called rotational fall. THUMS, with or without the safety-vest model, was placed on a ground mesh of solid elements with material properties representing dense sand, taken from [12] (LS-DYNA material model MAT_005: density $1.82e-6 \text{ kg/mm}^3$, bulk modulus $68.7e-3 \text{ GPa}$, shear modulus $1.00e-3 \text{ GPa}$). This position represented a rider doing a front flip and landing back first on the ground. The horse model was positioned to impact the THUMS' chest and stomach area to represent a worst-case scenario. Its initial velocity was estimated based on a riding velocity of 30 km/h when the horse hits a rigid obstacle at a point 50 cm away from its center of gravity. The initial rotational velocity of 6 rad/s was calculated by assuming that 70% of the translational kinetic energy transformed to rotational kinetic energy and the remaining 30% gave an initial translational velocity of 5 m/s.

To model a rider falling from a moving horse at a height of 1.5 meters, THUMS was positioned just above the ground and given an initial vertical velocity of 5.4 m/s and horizontal velocity of 15 km/h. Five different initial positions were generated by rotating the THUMS from the reference position in Fig. 4a around the global X- and Y-axes (Fig. 4b-e).

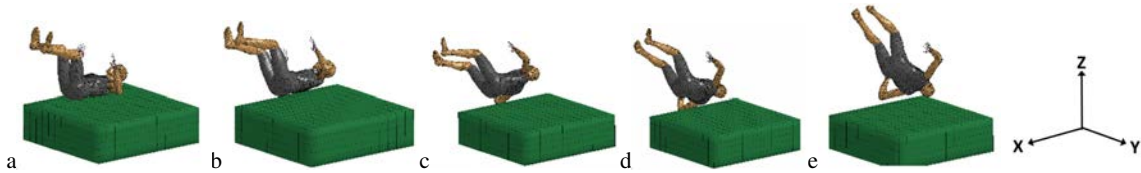


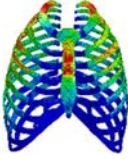
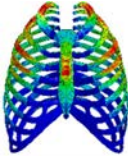
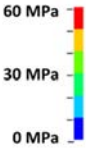
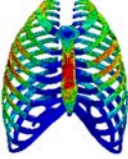
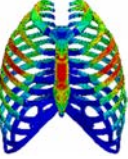
Fig. 4. THUMS initial position for the five different fall scenarios: (a) reference position; (b) 25° X-rotation; (c) 50° X-rotation; (d) 50° X rotation and -20° Y-rotation; (e) 50° X rotation and -40° Y-rotation.

3. Results and Discussion

3.1. When a rider is trampled by a horse, does the risk of injury vary with chest impact location?

Upon comparing the relative risk of rib fracture for different chest hoof impact locations, Table 2 illustrates that the injury criteria used change the relative predicted risk. The overall trend was that the superior hoof impact locations (#1-3) were associated with lower risk of injury compared to the more inferior locations (#4-6). The most lateral hoof impact locations (#1 and 4) were associated with an asymmetric rib cage deformation. The sternum impact locations (#3 and 6) produced symmetric deformation and larger local rib curvature, which gave higher risk of injury predictions for the tissue level criteria.

Table 2. AIS2+ risk of injury when the rider is trampled by the horse on different chest locations (not wearing a safety vest). The maximum predicted AIS2+ risk estimated using shear stress (τ), maximum principle strain (ϵ_1), DcTHOR, and Dmax. Images show the deformed ribcage with a contour plot of the average shear stress in each element, red color indicates $\tau > 60$ MPa and dark blue $\tau = 0$ MPa. Predicted rib fracture location (BR) is indicated for left (L) and right (R) side.

Location 1	Location 2	Location 3	
			
$\tau = 0\%$	$\tau = 20\%$	$\tau = 78\%$	
$\epsilon_1 = 8\%$	$\epsilon_1 = 82\%$	$\epsilon_1 = 87\%$	
DcTHOR= 1%	DcTHOR= 30%	DcTHOR= 1%	
Dmax = 53%	Dmax = 61%	Dmax = 74%	
BR: -	BR: R1	BR: L1 R1	
Location 4	Location 5	Location 6	
			
$\tau = 80\%$	$\tau = 1\%$	$\tau = 100\%$	
$\epsilon_1 = 39\%$	$\epsilon_1 = 23\%$	$\epsilon_1 = 55\%$	
DcTHOR= 22%	DcTHOR= 100%	DcTHOR= 26%	
Dmax = 91%	Dmax = 84%	Dmax = 84%	
BR: R6	BR: -	BR: L4 R4	

The maximum shear stress values vary from 56.2 to 74.6 MPa for the different locations, see fringe plots in Table 2. However, the risk curve used was very steep, and therefore, the predicted risk varied from 0 to 100%. This result is likely an exaggerated risk difference based on the cadaveric data used to create the risk curves. Also, it should be noted that sternum fractures are not predicted by the shear stress criterion, and it can be seen from the shear stress plots that the sternum had shear stress values above 60 MPa for several impact locations. The maximum principal strain criterion shows the same trends as the shear stress criterion (Table 2), predicting higher risk for impact locations close to the sternum. The maximum principal strain varies from 1.5 to 4.3% and the predicted risk from 8 to 87%. This range seems like a more realistic risk distribution and may point to toward a strain based criterion.

The global injury criteria, DcTHOR and Dmax both predicted low risk for the lateral most impact locations, which is expected because they are both based on chest compression in the anterior-posterior direction, rather than lateral components. Also, they are developed for frontal impacts and are not validated for lateral loading. DcTHOR takes into account asymmetric chest deflections, while Dmax only measures sternal compression at one point. Dmax varies from 26.6 to 34.7% and the predicted risk from 53 to 91%. DcTHOR maximum values range from 31.6 to 72.7 mm for the different impact locations, predicting risks from 1 to 100%. It is interesting to note that location 5 gets high risk with the global criteria, while the tissue criteria predicts the lowest risk. It is likely that the small lateral displacement of the sternum gives a less restricted rib deformation with lower stress and strain deformations, while the sternum and internal organs may be at risk because of a relatively large chest compression.

To conclude, it is evident that the AIS2+ risk of injury varies depending on the hoof impact location and that the answer to question #1 is yes. However, more research is needed to validate the biofidelity of the risk of injury criteria and their associated risk curves, especially for impacts with lateral components, to provide consistent results.

3.2. Does a safety-vest provide protection if the rider is kicked by a horse and does the protection vary with the violence of the hoof impact?

The AIS2+ risk of thoracic injury versus the momentum of the horse kick is plotted in Fig. 5. If the rider is not wearing a safety-vest (Fig. 5, solid lines), our results suggest that the risk of injury increases when the kick momentum is above 225 Ns. The safety-vest (Fig. 5, dashed lines) had a distinct risk reduction effect, because it offsets the momentum that the chest can withstand by approximately 125-175 Ns. Comparing the risk functions, the most conservative, in terms of risk prediction, was shear stress (τ). Note that Fig. 5 clearly shows the sharp shape of the shear stress risk curve. Dmax and maximum principal strain (ϵ_1) both have similar flatter risk curves up to 250 Ns, after that Dmax flattens out while the maximum principal strain increases. DcTHOR stands out by predicting much lower risk of injury compared to the other measures. It is not immediately obvious why this is the case, and warrants some caution with the use of DcTHOR. Hence, our results highlight again that more research is needed to understand why these injury criteria and their risk curves provide diverging results.

However, all four criteria predict a safety benefit for the safety-vest compared to not wearing a vest; and therefore, we can conclude that the answer to question #2 is yes. Also, as expected, the safety benefit of the vest was larger for hoof impacts with higher momentums up to a limit. We tentatively estimate the most beneficial range to be from 250 to 450 Ns. This range will be very dependent on the individual properties of each safety-vest and we suggest that commercial safety-vest should be investigated to determine their optimal range of performance. Such data would provide the consumer with valuable information in the choice between different safety-vest brands and models. FE HBMs seems to be a promising tool to optimize safety-vest material properties.

3.3. Can a safety-vest provide any benefit when the horse lands on top of the rider after a fall?

It was possible to simulate the rotational fall until a few tenths of a millisecond into the impact between the horse and rider. After that time the simulations terminated with negative volumes in finite elements because of the fatal chest deformation. Negligible differences in risk of injury were seen between the vested and non-vested models, because both of them estimated 100 % risk of sustaining an AIS2+ injury on all measures. The compression of the ribcage was 49 % for the non-vested and 51 % for the vested THUMS. Fig. 6 illustrates the end of the rotational fall event and visualizes the shear stress in the rib's cortical bone. The safety-vest did not provide any safety benefit when the rider was squashed under the horse, which was expected because of the large mass of the horse body. Therefore, we suggest to focus injury prevention on avoiding this type of accident rather than development of personal protection for the rider.

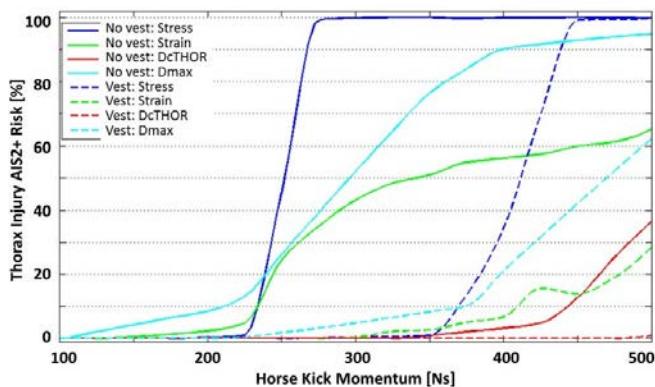


Fig. 5. Thorax AIS2+ risk of injury versus horse kick momentum measured with shear stress (blue lines), principal strain (turquoise line), DcTHOR (red line), and Dmax (green line) for THUMS without safety-vest (solid lines) and with safety-vest (dashed lines).

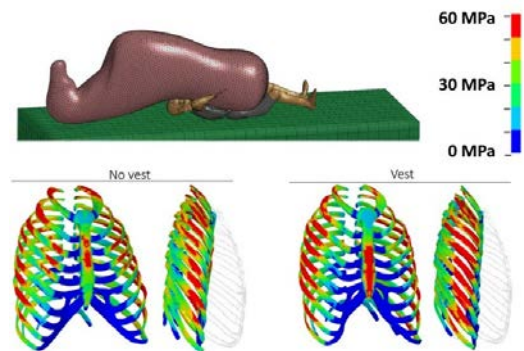


Fig. 6. Illustration of the rotational fall simulation showing THUMS and the horse body impactor model right before the simulation ended, with contour plots of the rib cage deformation and fringe plots of the average shear stress in the rib cage for both the vested and non-vested THUMS, including a light grey contour indicating the initial rib cage geometry.

3.4. How does the risk for thoracic injuries vary when the rider falls off the back of a horse at different angles?

Rib fractures were predicted for all five fall scenarios (Table 3), for a rider without a safety vest. We observed that the simulations where THUMS was falling with its head first tended to cause more fractured ribs (6-7 fractured ribs) compared to the more flat landings (2-4 fractured ribs). In the simulations with the head first, the THUMS rotated around the Y-axis while the flat landings produced X-rotation only. The predicted risk of AIS 2+ injury was 100 % for all fall simulations, with the maximum shear stress reaching values of 69 to 121 MPa. The next steps would be to analyze falls where the rider lands on uneven ground or

obstacles, like fences, and vary the fall height and riding speed. It is tempting to study the protective capacity of safety-vests using FE HBMs for these fall scenarios. FE simulations can be combined with optimization tools, thus introducing the opportunity to optimize the vest design and material properties for a range of accident scenarios.

Table 3. AIS2+ thoracic risk of injury predicted for five fall scenarios (for a rider without a safety vest) using shear stress (τ), maximum principle strain (ϵ), DcTHOR, and Dmax. Predicted rib fracture location (BR) is indicated for left (L) and right (R) side with rib number.

Fall scenario	τ	ϵ	DcTHOR	Dmax	BR
Reference position (Fig. 3a)	99%	55%	100%	85%	R4, R7
25 degrees X-rotation (Fig. 3b)	100%	82%	100%	85%	L7, R1, R7, R8
50 degrees X-rotation (Fig. 3c)	100%	99%	100%	61%	R1 R7 R8
50 degrees X rotation and -20 degrees Y-rotation (Fig. 3d)	100%	100%	100%	43%	R1 R2 R4 R6 R7 R8 R9
50 degrees X rotation and -40 degrees Y-rotation (Fig. 3e)	100%	92%	100%	7%	L1 R1 R4 R6 R7 R8

4. Conclusion

Simulations representing the most frequent equestrian accidents (falls, kicks and horse trample) were successfully performed with a commercially available FE HBM that was originally developed for vehicle safety applications. The thoracic risk of injury was evaluated with risk curves developed for an older population [4], which was supported by accident data that points out rib fractures as the major issue for older adult riders [3]. The simulations with a generic safety-vest for riders support that riders wearing safety-vests have protection against rib fractures from horse kicks. On the other hand, no benefit in rotational fall accidents where the rider is squashed under the horse were observed. FE HBM simulations can help set the agenda for injury prevention in equestrian sports by providing information on the potential of injury mitigation with personal protection for the rider. Efforts should be placed on development of personal protection for the rider or on avoidance of accident, like changing rules and improving release mechanisms for obstacles. FE HBMs have the potential to improve the safety benefit of riding vests through optimization of design and material properties, and to assess the safety benefit of vests designs currently on the market.

Acknowledgements

We thank Manuel Mendoza-Vazquez for support with the thoracic injury criteria and risk curves. This work was funded by the Chalmers' Area of Advance for Material Science: Sports and Technology and carried out within the environment at the SAFER Vehicle and Traffic Safety Center at Chalmers. The simulations were partly performed on resources at Chalmers Centre for Computational Science and Engineering (C3SE) provided by the Swedish National Infrastructure for Computing (SNIC).

References

- [1] Young JD, Gelbs JC, Zhu DS, Gallacher SE, Sutton KM, Blaine TA. Orthopaedic Injuries in Equestrian Sports. A Current Concepts Review. *The Orthopaedic Journal of Sports Medicine*, 2015; 3(9):1-7.
- [2] Sandiford N, Buckle C, Alao U, Davidson J, Ritchie J. Injuries associated with recreational horse riding and changes over the last 20 years: a review. *J R Soc Med* 2013;0:1-6.
- [3] Bilaniuk JW, Adams JM, DiFazio LT, Siegel BK, Allegra JR, Lujan JJ, Durling-Grover R, Pawar J, Rolandelli RH, Németh ZH. Equestrian Trauma: Injury Patterns Vary among Age Groups. *Am Surg*. 2014; 80:396-402.
- [4] Mendoza-Vazquez M, Brolin K, Davidsson J, Wismans J. Human rib response to different restraint systems in frontal impacts: a study using a human body model, *International Journal of Crashworthiness*, 2013;18(5):516-529.
- [5] Mendoza-Vazquez M, Davidsson J, Brolin K. Construction and evaluation of thoracic risk of injury curves for a finite element human body model in frontal car crashes. *Accident Analysis and Prevention*. 2015;85:73-82.
- [6] Mendoza-Vazquez M, Jakobsson L, Davidsson J, Brolin K, Östmann M. Evaluation of Thoracic Injury Criteria for THUMS Finite Element Human Body Model Using Real-World Crash Data. *IRCOBI International Research Council on the Biomechanics of Injury*, 10-12 September, Berlin, Germany. 2014; 528-541.
- [7] Kleinberger M, Sun E, Eppinger R, Kuppa S, Saul R. Development of Improved Injury Criteria for the Assessment of Advanced Automotive Restraint Systems. *NHTSA*. 1989.
- [8] Davidsson, J, Carrol, J, Hynd, D, Lecuyer, E, Song, E, Trosseille, X, Eggers, A, Sunnevång, C, Praxl, N, Martinez, L, Lemmen, P, Been, B. Development of risk of injury functions for use with the THORAX Demonstrator; an updated THOR. *IRCOBI International Research Council on the Biomechanics of Injury*, 10-12 September, Berlin, Germany. 2014; 359-376.
- [9] www.smartpakequine.com/protective-vests-and-safety-824pc. Smartpakequine. Accessed on August 2015.
- [10] Dynaexamples.com/sph/foam. Ls-dyna examples of foam material modelling. Accessed on August 2015.
- [11] MatWeb.com. Material property data for nylon 6, unreinforced. Accessed on August 2015.
- [12] Fasanella EL, Jackson KE, Kellas S. Soft Soil Impact Testing and Simulation of Aerospace Structures. *10th International LS-DYNA User's Conference*; 8-10 Jun. 2008; Dearborn, MI; United States.